Inflammation, Vol. 45, No. 6, December 2022 (© 2022)
https://doi.org/10.1007/s10753-022-01695-0

ORIGINAL ARTICLE

Gut-Derived Exosomes Induce Liver Injury After Intestinal Ischemia/Reperfusion by Promoting Hepatic Macrophage Polarization

Jin Zhao[1] , Xiao-Dong Chen[1] , Zheng-Zheng Yan[1] , Wen-Fang Huang[1] , Ke-Xuan Liu[1,2] and Cai Li[1,2]

Received 26 February 2022; accepted 31 May 2022

Abstract— Liver injury induced by intestinal ischemia/reperfusion (I/R) is accompanied by the polarization of Kupffer cells, which are specialized macrophages located in the liver. However, the causes of hepatic macrophage polarization after intestinal I/R remain unknown. This study investigated whether gut-derived exosomes contribute to the pathogenesis of liver injury triggered by intestinal I/R in a murine model and explored the underlying mechanisms. Intestinal I/R models were established by temporally clamping the superior mesenteric arteries of mice. Exosomes were isolated from the intestinal tissue of mice that underwent intestinal I/R or sham surgery according to a centrifugation-based protocol. Exosomes were co-cultured with RAW 264.7 macrophages or injected intravenously in mice. Liposomal clodronate was administered intraperitoneally to deplete the macrophages. Macrophage polarization was determined by flow cytometry, immunohistochemistry, and quantitative polymerase chain reaction. Liver injury was assessed by histological morphology and increased serum aspartate aminotransferase and alanine aminotransferase levels. Exosomes from mice intestines subjected to I/R (IR-Exo) promoted macrophage activation *in vitro*. Intravenous injection of IR-Exo caused hepatic M1 macrophage polarization and led to liver injury in mice. Depleting macrophages ameliorated liver injury caused by intestinal I/R or the injection of IR-Exo. Furthermore, inhibiting exosome release improved intestinal injury, liver function, and survival rates of mice subjected to intestinal I/R. Our study provides evidence that gut-derived exosomes induce liver injury after intestinal I/R by promoting hepatic M1 macrophage polarization. Inhibition of exosome secretion could be a therapeutic target for preventing hepatic impairment after intestinal I/R.

KEY WORDS: intestinal ischemia/reperfusion; liver; exosome; macrophage polarization.

Jin Zhao and Xiao-Dong Chen contributed equally to this work.

[1]Department of Anesthesiology, Nanfang Hospital, Southern Medical University, 1838 Guangzhou Ave N, Guangzhou 510515, China
[2]To whom correspondence should be addressed at and Department of Anesthesiology, Nanfang Hospital, Southern Medical University, 1838 Guangzhou Ave N, Guangzhou, 510515, China. Email: liukexuan705@163.com; 10414985@qq.com

INTRODUCTION

Intestinal ischemia/reperfusion (I/R) injury is a serious but common clinical occurrence caused by a number of pathophysiological factors, including superior mesenteric artery occlusion, abdominal and thoracic vascular surgery, cardiopulmonary bypass, or small intestine

transplantation, resulting in severe local and remote tissue injury and subsequent organ dysfunction, and has been extensively studied [1–3]. This common problem encountered in a broad range of clinical settings can create a life-threatening abdominal emergency with a survival rate of less than 50% [4]. Liver injury is a component of multiple organ dysfunction syndrome triggered by intestinal I/R, which results in high mortality, and macrophages have an essential role [5]. Hepatic macrophages are highly plastic and can be activated and polarized into classically activated macrophages (M1 macrophages) or alternatively activated macrophages (M2 macrophages) in different microenvironments. Accumulating evidence has shown that M1 and M2 macrophage polarization participates in the process of several types of hepatic diseases, including acute liver failure, viral hepatitis, nonalcoholic steatohepatitis, liver fibrosis, and hepatocyte cancer [6]. Recent studies have found that macrophage activation and M1 polarization are also involved in the development of liver injury after intestinal I/R [5, 7]. The release of danger-associated molecular patterns from enterocytes via portal circulation promotes Kupffer cell polarization and contributes to liver injury after intestinal I/R [7]. However, the mechanisms by which intestinal-derived inflammatory signals spread to macrophages during the development of liver injury after intestinal I/R are not fully understood.

Exosomes are nanosized vesicles released by nearly all types of cells under normal and pathological conditions into the extracellular space and circulation. Exosomes are important mediators of communication between cells and organs. Intestinal epithelial cell-released exosomes are capable of regulating the differentiation and activity of immune cells, such as dendritic cells [8]. Furthermore, gut epithelial cell-derived exosomes could be released into the mesenteric lymph, trigger acute lung injury, and mediate immunosuppression in hemorrhagic shock [9, 10]. Exosome-like nanoparticles from intestinal mucosal cells migrate to the liver and affect natural killer T cells [11]. However, the relationship between intestinal-derived exosomes and hepatic injury after intestinal I/R needs to be explored.

We hypothesized that exosomes released after intestinal I/R are endogenous signals that lead to acute liver injury by promoting M1 macrophage polarization. During the present study, we extracted exosomes from the intestinal tissue of mice that underwent intestinal I/R or sham surgery. Then, we explored the effects of these intestinal-derived exosomes on the liver after intestinal I/R. We demonstrated that intestinal exosomes can be engulfed by hepatic macrophages, thereby causing M1 macrophage polarization, hepatic enzyme elevation, and liver tissue impairment in mice subjected to intestinal I/R.

METHODS

Animal Models and Treatments

This study was approved by the Institutional Animal Care and Use Committee of Southern Medical University in Guangzhou, China, and complied with the national guidelines for the treatment of animals. Six- to eight-week-old specific pathogen-free male C57BL/6 mice weighing 20 ± 2 g were kept in a facility with controlled temperature and humidity conditions under 12-h cycles of light and darkness. The mice freely accessed food and water. Before surgery, the mice were fasted for 12 h and had free access to water only. Surgical procedures for intestinal I/R modeling were performed under general anesthesia and sterile conditions. The mice were anesthetized with pentobarbital (45 $mg \cdot kg^{-1}$) injected intraperitoneally and kept warm on a thermal pad. An abdominal midline incision was created, the superior mesenteric artery was identified and clamped for 60 min, and the incision was closed after removal of the clamp to initiate reperfusion. After 6 h of reperfusion, the mice were anesthetized and the intestine, liver, and blood were harvested.

To inhibit exosome release, the mice were randomly allocated to three groups: the sham group without superior mesenteric artery clamping; the I/R group; and the I/R + GW4869 group, these two groups of mice pretreated with phosphate-buffered saline (PBS) and 2.5 $mg \cdot kg^{-1}$ GW4869 (Sigma-Aldrich, USA), intraperitoneal injection, respectively, at 12 h before ischemia and at the beginning of intestinal reperfusion.

For exosome treatment, mice were randomly divided into three groups: the PBS group pretreated with 200 µl PBS; the Sham-Exo group pretreated with 100 µg exosomes (200 µl) from the sham group small intestine; and the IR-Exo group pretreated with 100 µg exosomes (200 µl) from the I/R group small intestine, PBS, and exosome injection via the orbital venous sinus.

To deplete macrophages, mice were randomly grouped into four groups. The I/R + clodronate (Clod) group and I/R + control (Con) group mice received 200 µl liposomal clodronate (Yeasen, China) and an equal volume of liposome PBS (empty liposomes) intraperitoneally, respectively, at 24 h before intestinal ischemia.

The IR-Exo + clod group and IR-Exo + Con group mice also received liposomal clodronate or liposome PBS as described before exosomes from intestinal I/R surgery were administered via intravenous injection. After reperfusion or exosome treatment for 6 h, the mice were euthanized and their organs were harvested.

Survival Analysis

Seventy mice were randomly assigned to three experimental groups: sham group ($n = 10$); I/R group ($n = 30$); and I/R + GW4869 group ($n = 30$). The vital signs of the mice were monitored for 3 days after the onset of intestinal reperfusion.

Cell Culture

The murine RAW 264.7 macrophage cell line was supplied by ATCC. Murine RAW 264.7 cells in a six-well plate were maintained in DMEM enriched with 10% fetal bovine serum under 5% CO_2 at 37 °C.

Exosome Treatment of Cells

Exosomes (5 μg·ml^{-1}) derived from intestinal tissues in the sham and I/R groups were added to the cell culture medium for 12 h.

Exosome Uptake Assay

Exosomes and cells were labeled with PKH67 (Sigma-Aldrich, USA) and PKH26 fluorescent dye (Sigma-Aldrich, USA), respectively, according to the instructions of the manufacturer. Co-localization of the PKH67-labeled exosomes and PKH26-labeled RAW 264.7 cells for 12 h was observed using fluorescence microscopy.

Statistical Analysis

Data analysis was performed using GraphPad Prism software version 8 (GraphPad Software, San Diego, CA, USA). Quantitative values are given as the means ± standard error of mean (SEM). Two continuous normally distributed variables were compared by unpaired *t*-test. The Mann–Whitney *U* test was used to compare the means of two groups of variables that were not normally distributed. The log-rank test was used for survival analyses. Statistical significance was set at $P < 0.05$.

The remaining methods are detailed in the supplementary materials.

RESULTS

Characterization and Quantification of Intestine-Derived Exosomes

The exosomes were isolated and purified using a standard protocol of serial differential centrifugation and ultracentrifugation steps after grinding and enzymatic digestion of intestinal tissues. Western blotting showed that exosomal protein markers CD9, CD63, and CD81 were enriched at a density of 1.12 to 1.18 g·ml^{-1}, whereas calnexin, an indicator of intracellular component contamination, was not found (Fig. 1a), as reported previously [12]. Transmission electron micrographs confirmed the presence of exosomes approximately 30 to 150 nm in diameter as the typical cup-shaped vesicles (Fig. 1b). Nanoparticle tracking analysis revealed that exosomes from sham and I/R mice had mean particle sizes of 39.5 nm and 36.4 nm, respectively (Fig. 1c).

IR-Exo Causes RAW 264.7 Macrophage Activation

To explore the direct effect of intestinal exosomes on RAW 264.7 macrophages, we applied PKH67-labeled intestinal exosomes to RAW 264.7 macrophages. Images obtained by fluorescence microscopy confirmed that both types of exosomes were internalized in RAW 264.7 macrophages after 12 h of co-incubation (Fig. 2a). Both exosomes in group Sham-Exo and IR-Exo were taken up by about 65% of cultured RAW 264.7 cells (Fig. 2b). We analyzed changes in RAW 264.7 macrophages pro-inflammatory gene expression after stimulation with intestinal exosomes. IR-Exo treatment remarkably upregulated the mRNA levels of TNF-α, IL-1β, IL-6, and iNOS (Fig. 2c–f). Phosphorylation of NF-κB (p65) and IκB-α, and degradation of total IκB-α, which indicates activation of NF-κB signaling, increased in the IR-Exo-treated RAW 264.7 cells compared with sham-Exo or PBS (Fig. 2g–k), although the p-IkB-alpha showed no significantly difference between S-Exo and IR-Exo group ($p = 0.1153$). The results showed that IR-Exo promoted NF-κB-mediated inflammation signaling and activated macrophages.

IR-Exo Causes Macrophage Infiltration, M1 Polarization, and Liver Inflammation in Mice

To investigate whether exosomes could reach the liver and activate macrophages *In vivo*, we injected intestinal exosomes in healthy mice. PKH26 and FITC double-positive cells represent the number of macrophages in the phagocytic exosomes, and the ratios of PKH26 and FITC double-positive cells/PKH26 single-positive cells reflect the ability of macrophages to phagocytose exosomes (Fig. 3b, c). Exosomes from the intestinal I/R and sham group were mobilized to the liver parenchyma 6 h after injection (Fig. 3a, b) and were mainly taken up by F4/80$^+$ hepatic macrophages as determined by immunofluorescence (Fig. 3a, c). The injection of IR-Exo resulted in increased F4/80$^+$ macrophage infiltration (Fig. 3d, e). M1 polarization in the liver was detected using flow cytometry and immunohistochemistry. M1 markers CD86 and iNOS were significantly expressed in the IR-Exo group (Fig. 3f–m). The expression of pro-inflammatory cytokine (IL-1β, IL-6, IL-18, CCL2, and CXCL9) mRNA in the liver was also increased by IR-Exo group. In contrast, Sham-Exo injection did not cause a liver inflammatory response (Fig. 3n–r).

Fig. 2 IR-Exo causes RAW 264.7macrophage activation. **a**, **b** RAW 264.7 macrophages were incubated with PKH67 labeled intestinal-derived exosomes harvested from sham and intestinal I/R surgery for 12 h. Representative pictures of RAW 264.7 macrophages that had internalized intestinal-derived exosome analyzed by fluorescence microscopy. Cell membrane was stained using PKH26, and the nuclei were DAPI. Color-merged image shows DAPI in blue, PKH26 in red, and PKH67-labeled exosomes in green. Scale bar is 50 μm. **c**–**f** The relative mRNA level of TNF-α, IL-6, IL-1β, iNOS in RAW 264.7 macrophages was analyzed by RT-PCR. **g**–**k** Representative image and protein expression levels of p-IkB-α, IkB -α, p-P65, total p65 by western blotting analysis. Data are presented as the mean ± SEM. * $P<0.05$, ** $P<0.01$, *** $P<0.001$ compared with PBS group; # $P<0.05$, ## $P<0.01$, ### $P<0.001$ compared with Sham-Exo group; $n=3$ mice per group. IL: interleukin, iNOS: inducible nitric oxide synthase, NF-κB: nuclear factor kappa-B, TNF: tumor necrosis factor, IR-Exo: exosomes from mice intestines subjected to I/R surgery, Sham-Exo (S-Exo): exosomes from mice intestines subjected to sham surgery.

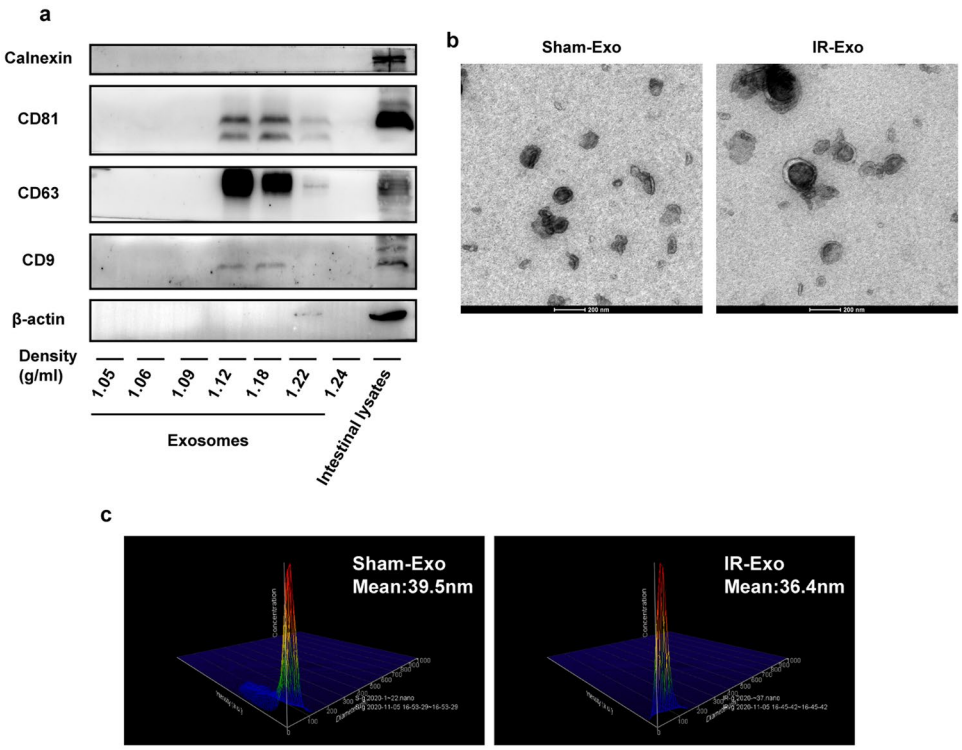

Fig. 1 Characterization and quantification of intestinal-derived exosomes. **a** The exosomes from intestines were loaded on a continuous sucrose gradient, and the fractions and total intestinal lysates were immunoblotted with corresponding antibodies. **b** Electron micrographs of purified exosomes from the intestines. Scale bars is 200 nm. **c** The size of intestinal exosomes analyzed by NTA. NTA: nanoparticle tracking analysis, IR-Exo: exosomes from mice intestines subjected to I/R surgery, Sham-Exo (S-Exo): exosomes from mice intestines subjected to sham surgery.

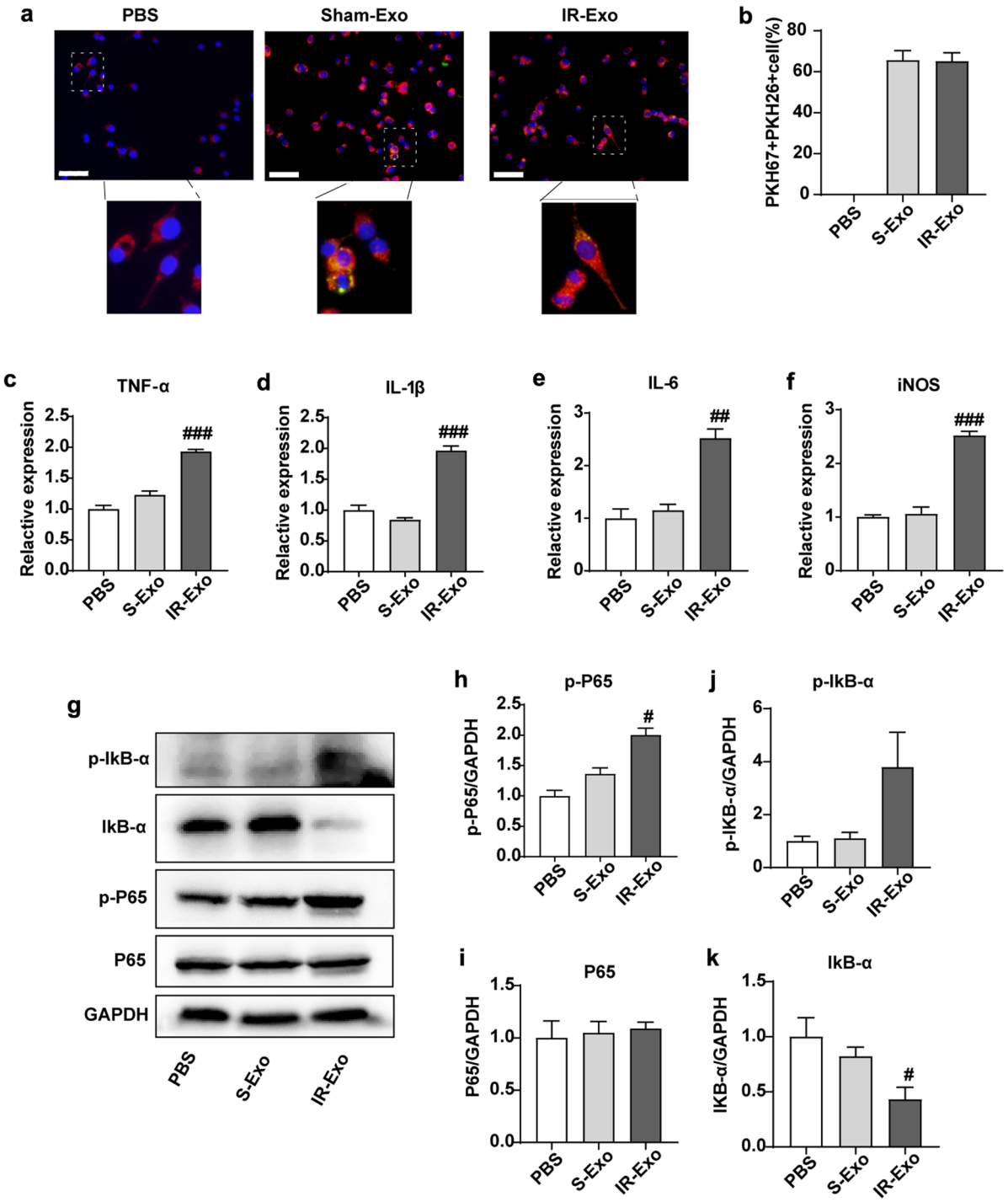
a
PBS
Sham-Exo
IR-Exo
b
PKH67+PKH26+cell(%)
80
60
40
20
0
PBS
S-Exo
IR-Exo
c
TNF-α
Relative expression
2.5
2.0
1.5
1.0
0.5
0.0
###
PBS
S-Exo
IR-Exo
d
IL-1β
Relative expression
2.5
2.0
1.5
1.0
0.5
0.0
###
PBS
S-Exo
IR-Exo
e
IL-6
Relative expression
3
2
1
0
##
PBS
S-Exo
IR-Exo
f
iNOS
Relative expression
3
2
1
0
###
PBS
S-Exo
IR-Exo
g
p-IkB-α
IkB-α
p-P65
P65
GAPDH
PBS
S-Exo
IR-Exo
h
p-P65
p-P65/GAPDH
2.5
2.0
1.5
1.0
0.5
0.0
#
PBS
S-Exo
IR-Exo
j
p-IkB-α
p-IKB-α/GAPDH
6
4
2
0
PBS
S-Exo
IR-Exo
i
P65
P65/GAPDH
1.5
1.0
0.5
0.0
PBS
S-Exo
IR-Exo
k
IkB-α
IKB-α/GAPDH
1.5
1.0
0.5
0.0
#
PBS
S-Exo
IR-Exo

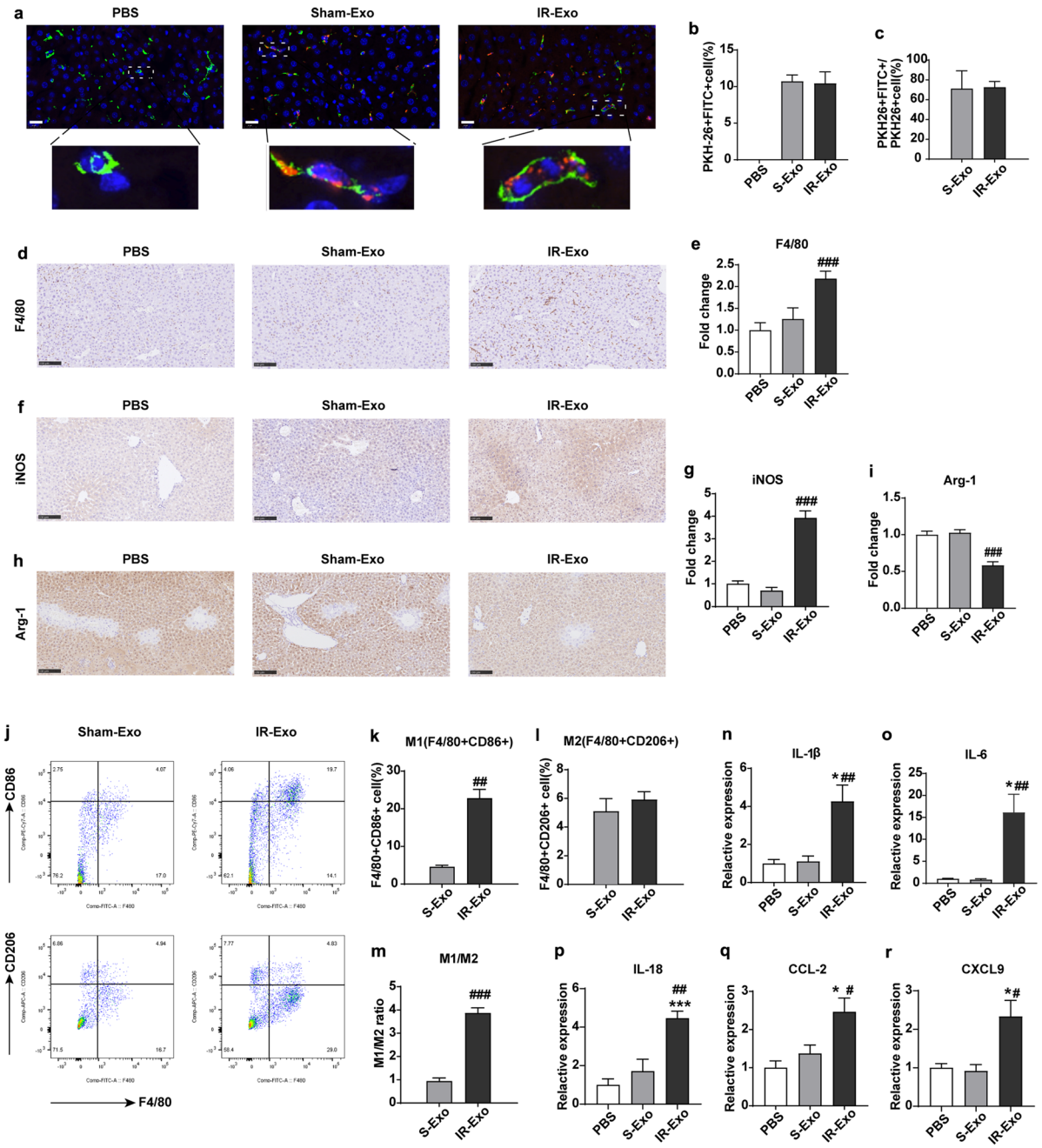

Fig. 3 IR-Exo causes macrophage infiltration, M1 polarization in mice. **a** Immunofluorescence co-localization of the PKH26 labeled exosomes and FITC-F4/80 labeled hepatic macrophages, and **b** the proportion of PKH26 + FITC + cells and **c** PKH26 + FITC + /PKH26 + cell. **d**–**i** Representative images of immunohistochemical staining with F4/80 (**d**), iNOS (**f**) and Arg-1 (**h**) antibody in the liver. Scale bar is 100 μm. **e**, **g**, **i** The fold change of the numbers of positive loci were calculated. **j**–**m** The quantification of CD86 + F4/80 + (M1) and CD206 + F4/80 + (M2) and the M1/M2 ratio of macrophage was measured by flow cytometry. **n**–**r** Relative mRNA expression levels of IL-1β, IL-6, IL-18, CCL-2 and CXCL9 were analyzed by RT-PCR. Data presented as mean ± SEM.* $P < 0.05$, ** $P < 0.01$, *** $P < 0.001$ compared with PBS group; #$P < 0.05$, ##$P < 0.01$, ###$P < 0.001$ compared with Sham-Exo group; n = 3–5 mice per group. ALT: alanine aminotransferase, Arg-1: Arginase-1, AST: aspartate aminotransferase, CCL: Chemokine C–C Motif Ligand, CXCL: Chemokine C-X-C motif Ligand, IL: interleukin, iNOS: inducible nitric oxide synthase, IR-Exo: exosomes from mice intestines subjected to I/R surgery, Sham-Exo (S-Exo): exosomes from mice intestines subjected to sham surgery.

Altogether, these results demonstrate that IR-Exo can induce M1 macrophage polarization and liver inflammation.

IR-Exo Induced Liver Injury in Mice

Next, we tested the biological effects of intestinal exosomes on liver tissue of mice. The results indicated that the histological score of the liver in mice injected with IR-Exo was significantly higher than that of mice injected with PBS and Sham-Exo (Fig. 4a, b). Additionally, compared with the Sham-Exo group, the levels of serum ALT and AST in IR-Exo were significantly increased (Fig. 4c, d). These results suggest that IR-Exo, but not Sham-Exo, can cause liver damage.

Macrophage Depletion Ameliorated Exosome-Mediated Liver Injury After Intestinal I/R

To verify whether hepatic macrophages are responsible for exosome-mediated liver injury, liposomal clodronate was used to deplete macrophages. As shown by immunohistochemistry for F4/80, almost all macrophages in the liver in the clodronate group were depleted compared with the empty liposome groups (Fig. 5a). Macrophage depletion could reverse intestinal I/R-triggered liver injury and exosomes from I/R surgery-mediated liver injury, which was indicated by recovered lesions with lower Suzuki scores (Fig. 5b, c), decreased serum

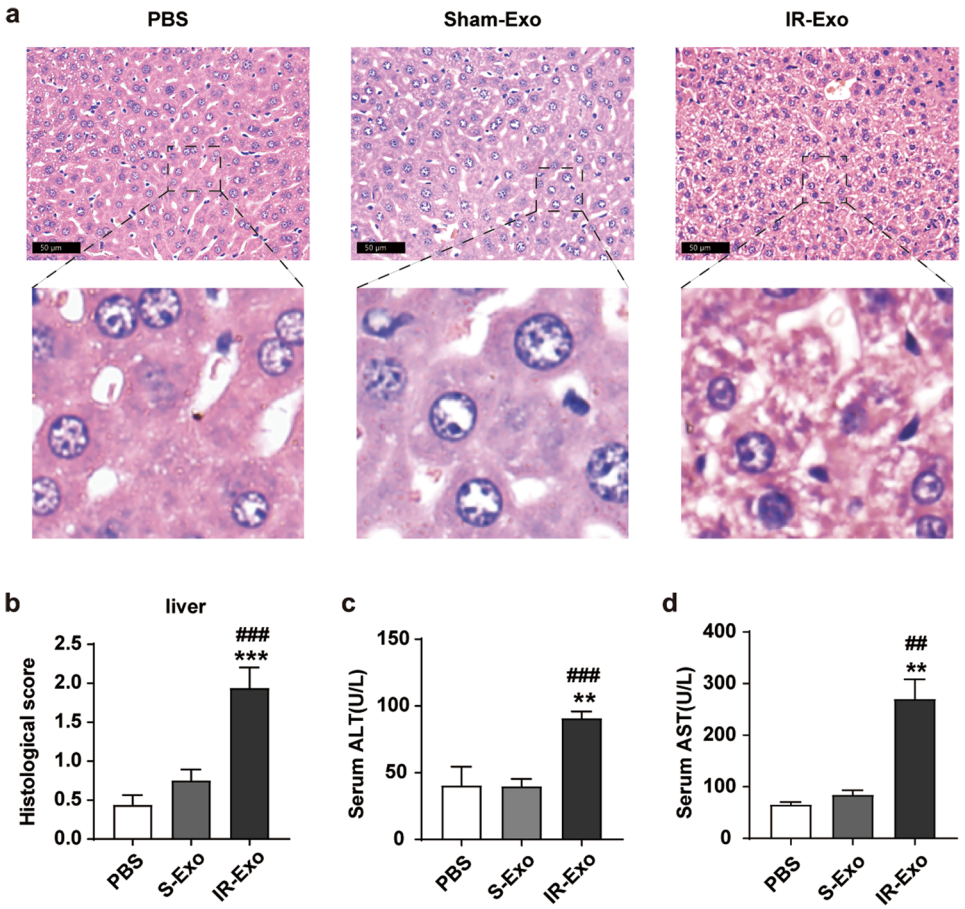

Fig. 4 IR-Exo causes liver injury in mice. **a** Representative images of liver histology stained with HE after exosomes injection. Injection of IR-Exo caused liver damage that was characterized by sinusoidal congestion and vacuolization, whereas injection of Sham-Exo resulted in mild tissue damage. **b** Liver injury was assessed by Suzuki's criteria. **c**–**d** Levels of ALT and AST in the sera. Data presented as mean ± SEM.* $P < 0.05$, ** $P < 0.01$, *** $P < 0.001$ compared with PBS group; # $P < 0.05$, ## $P < 0.01$, ### $P < 0.001$ compared with Sham-Exo group; $n = 3$–5 mice per group. ALT: alanine aminotransferase, AST: aspartate aminotransferase, IR-Exo: exosomes from mice intestines subjected to I/R surgery, Sham-Exo (S-Exo): exosomes from mice intestines subjected to sham surgery.

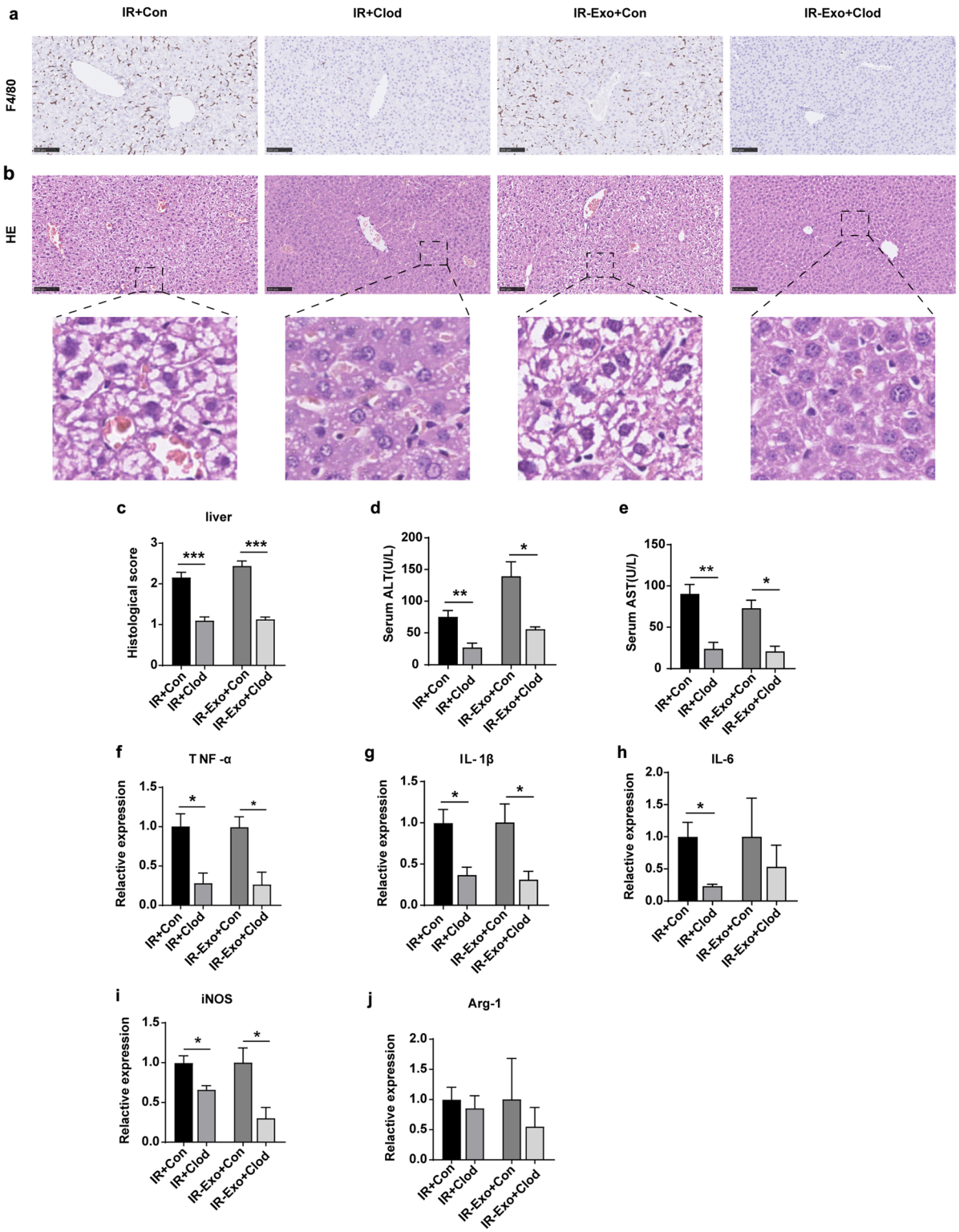
a
IR+Con
IR+Clod
IR-Exo+Con
IR-Exo+Clod
F4/80
b
HE
c
liver
Histological score
d
Serum ALT(U/L)
e
Serum AST(U/L)
f
TNF-α
Relactive expression
g
IL-1β
h
IL-6
i
iNOS
j
Arg-1

◀ **Fig. 5** Macrophage depletion ameliorated exosomes-mediated liver injury following intestinal I/R. **a** Immunohistochemical examination was performed by F4/80. **b–c** Representative histological staining using HE was demonstrated. **d–e** Levels of ALT and AST in the sera. **f–j** Relative mRNA expression levels of TNF-α, IL-1β, IL-6, iNOS, and Arg-1 were measured by RT-PCR. Data presented as mean ± SEM. $n = 3–5$ mice per group. * $P < 0.05$, ** $P < 0.01$, *** $P < 0.001$. ALT: alanine aminotransferase, Arg-1: Arginase-1, AST: aspartate aminotransferase, HE: hematoxylin and eosin, IL: interleukin, iNOS: inducible nitric oxide synthase, TNF: tumor necrosis factor.

ALT and AST levels (Fig. 5d, e), and the expression levels of TNF-α, IL-1β, and iNOS mRNA in the liver (Fig. 5f–j).

Inhibition of Exosome Release Reduces Macrophage Infiltration, M1 Polarization, and Liver Inflammation After Intestinal I/R

To investigate whether inhibition of exosome release could reduce pro-inflammation of hepatic macrophages *In vivo*, GW4869 was used to block the release of exosomes in mice. Immunohistochemical staining of liver tissue to explore the impact of GW4869 treatment on macrophage infiltration showed that macrophages (marked by F4/80) increased in the liver of the intestinal I/R mice in contrast with the sham group and were remarkably diminished after GW4869 injection (Fig. 6a, b). We isolated hepatic macrophages and performed flow cytometry to verify the polarization of macrophages via GW4869 modulation. The data demonstrated that intestinal I/R resulted in remarkably increased $CD86^+F4/80^+$ and $CD206^+F4/80^+$ macrophages in the liver tissue, especially $CD86^+F4/80^+$ macrophages. Therefore, the ratio of M1/M2 macrophages remarkably increased in intestinal I/R mice compared to sham and GW4869-pretreated mice (Fig. 6g–j). GW4869 administration decreased the shift toward the M1 phenotype. The iNOS (M1-related markers) protein expression was reduced and Arg-1 (M2-related markers) protein expression was increased in the GW4869 group mice (Fig. 6c–f). Similar to the suppressive effects on macrophage M1 polarization, GW4869 remarkably diminished the expression of pro-inflammatory cytokine genes (IL-1β, IL-6, IL-18, and CCL2) (Fig. 6k–n). The results indicated that inhibition of exosome release could reduce M1 macrophage polarization and liver inflammation.

Inhibition of Exosome Release Improves the Survival of Mice and Alleviates Liver Injury After Intestinal I/R

To validate the functional link between exosome secretion and intestinal I/R-triggered liver injury *In vivo*, mice were pretreated with GW4869. The protective effect of GW4869 was observed after 4 h of reperfusion. At 72 h after I/R surgery, only 10% of mice in the I/R group survived, whereas 56.7% of mice in the I/R + GW4869 group survive (Fig. 7a). Intestinal I/R triggered devastating ileum injury manifesting as massive epithelial lifting on the sides of villi and hemorrhage in the lamina propria. Administration of GW4869 reduced these local injuries (Fig. 7b). There were dramatic differences in the intestinal injury scores of the I/R and I/R plus GW4869 groups (Fig. 7c). Accordingly, intestinal I/R triggered liver injury with marked hepatocyte vacuolization and congestion. However, GW4869 alleviated this liver injury (Fig. 7b). A semi-quantitative assessment of liver damage scores demonstrated the mitigation of intestinal I/R-triggered liver injury by GW4869 (Fig. 7d). Additionally, liver enzymes were increased in response to intestinal I/R and diminished by GW4869 (Fig. 7e, f). Collectively, these results illustrate that GW4869-induced blockade of exosome production improves survival and mitigates intestinal I/R-triggered liver injury.

DISCUSSION

During this study, we demonstrated that intestinal I/R induces liver injury characterized by increased hepatic enzymes, increased M1 macrophage infiltration, and aggravated liver inflammation. Our study also showed that IR-Exo caused liver injuries in mice that were similar to those caused by intestinal I/R. Furthermore, IR-Exo can be encapsulated and activate macrophages into M1 states both *in vitro* and i*n vivo* and contribute to liver injury. The macrophage depletion study further confirmed that hepatic M1 macrophage polarization is responsible for gut-derived exosomes mediating liver injury after intestinal I/R. Inhibition of exosome secretion reversed M1 macrophage polarization and liver injury after intestinal I/R.

The gut has been identified as an initiator of the onset of multiple organ dysfunction. Free radicals, inflammatory mediators produced by the gut, and bacteria or enterotoxin translocation from the lumen or the interstitial

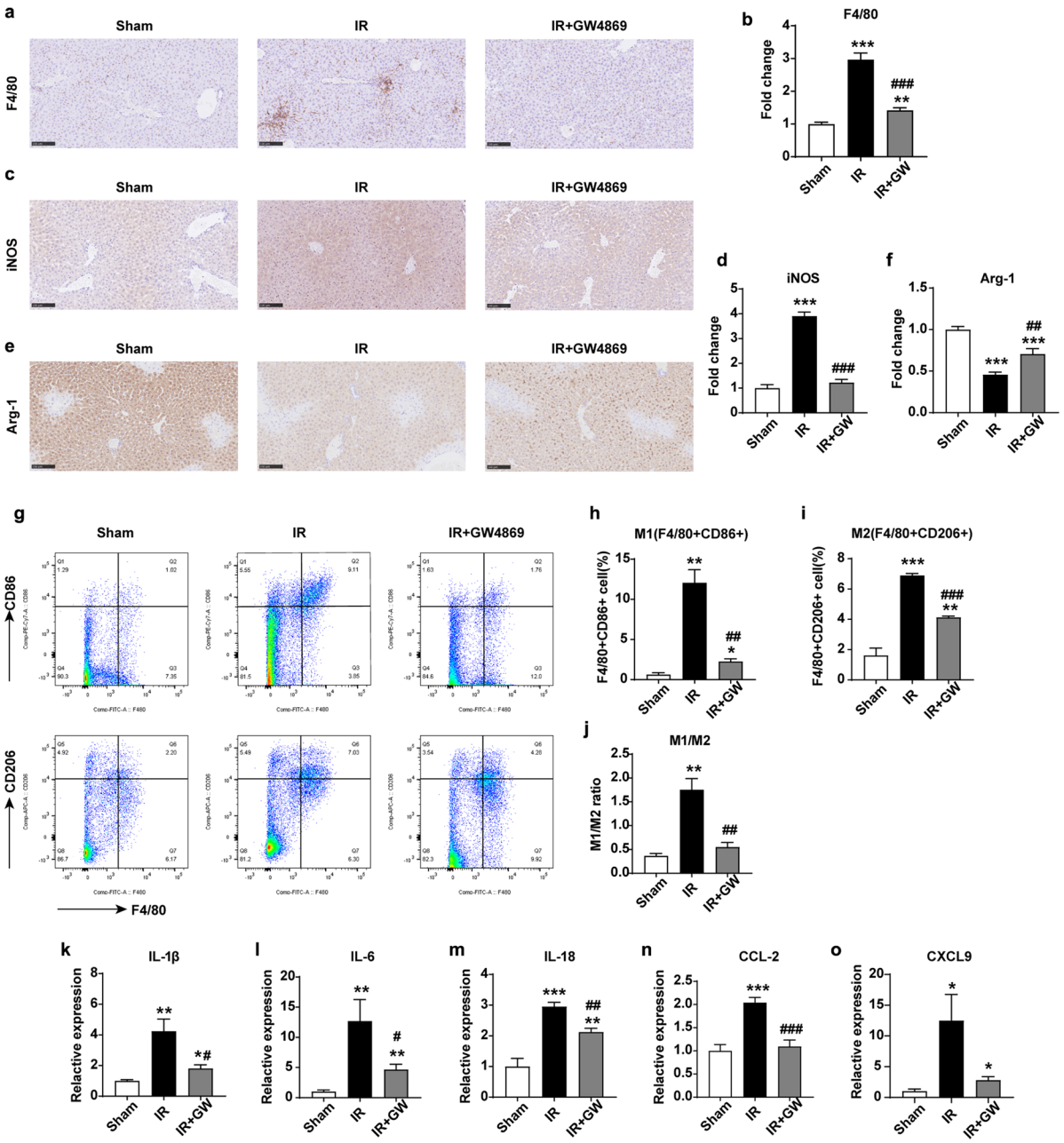

Fig. 6 Inhibition of exosomes release reduce macrophage infiltration and M1 polarization, and liver inflammation after intestinal I/R. **a**–**f** Representative images of immunohistochemical staining with F4/80, iNOS and Arg-1 antibody in the liver. Scale bar is 100 μm. The fold change of the numbers of positive loci among three groups were calculated. **g**–**j** The quantification of CD86 + F4/80 + (M1) and CD206 + F4/80 + (M2) and the M1/M2 ratio of macrophage was detected by flow cytometry. **k**–**o** Relative mRNA expression levels of IL-1β, IL-6, IL-18, CCL-2, and CXCL9 were measured by RT-PCR. Data presented as mean ± SEM. * $P < 0.05$, ** $P < 0.01$, *** $P < 0.001$ compared with sham group; # $P < 0.05$, ## $P < 0.01$, ### $P < 0.001$ compared with IR group; $n = 3$–5 mice per group. Arg-1: Arginase-1, CCL: Chemokine C–C Motif Ligand, CXCL: Chemokine C-X-C motif Ligand, IL: interleukin, iNOS: inducible nitric oxide synthase, GW: GW4869.

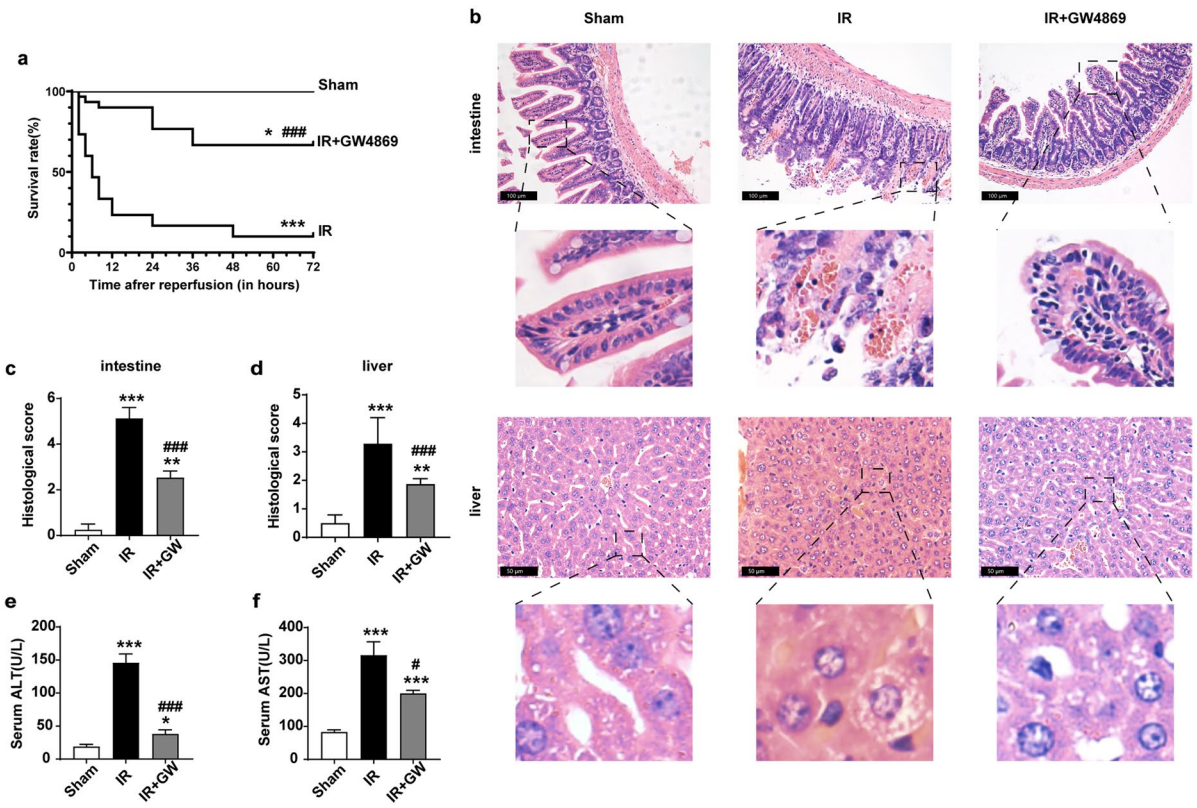

Fig. 7 Inhibition of exosomes release improves survival of mice and alleviates liver injury after intestinal I/R. **a** Treatment with GW4869 significantly improved survival after a 1-h intestinal I/R. **b** Representative images of HE staining ileum and liver tissues from the sham, IR and IR + GW4869 groups are shown. **c**–**d** The extent of intestinal damage and liver injury was evaluated using modified Chiu's score and Suzuki's criteria, respectively. **e**–**f** The ALT and AST levels in the sera. Data presented as mean ± SEM. $^{*}P < 0.05$, $^{**}P < 0.01$, $^{***}P < 0.001$ compared with sham group; $\#P < 0.05$, $\#\#P < 0.01$, $\#\#\#P < 0.001$ compared with IR group; $n = 5$ mice per group. ALT: alanine aminotransferase, AST: aspartate aminotransferase, HE: hematoxylin and eosin, GW: GW4869.

space of the affected bowel into lymph nodes and the bloodstream during intestinal I/R result in injuries to the remote organs, including the lung [13], liver [14], heart [15], kidney [16], and brain [17]. Because of portal venous drainage, the liver appears to be the first organ affected by toxic agents released from the intestine after intestinal I/R. Moreover, when the liver is compromised, these mediators can enter the systemic circulation, leading to a cascade of progressive organ system decay. Liver damage after intestinal I/R may be attributed to a mechanism involving increments in histone aggregation and neutrophil extracellular trap formation [18], the release of HMGB1 from necroptotic enterocytes [7], NLRP3 inflammasome activation [19], excessive generation of oxygen free radicals [20] and cytokines/chemokines [21], and hepatic microvascular dysfunction triggered by leukocyte adhesion [22]. Our results also confirmed that intestinal I/R triggered liver injury with marked hepatocyte vacuolization, congestion, and increased hepatic enzymes accompanied by increased M1 macrophage infiltration and aggravated inflammation of the liver.

Intravenous injection was used to simulate the effects of intestinal exosomes on other peripheral organs. We treated healthy mice with purified intestinal exosomes from sham and intestinal I/R surgery. Our results indicated that IR-Exo initiated in mice contributed to liver injury and macrophage activation into M1 states, similar to intestinal I/R. These data illustrate that intestinal exosomes participate in the pathogenesis of liver injury triggered by intestinal I/R.

Exosomes are mediators of intercellular communication and modify recipient cells biology. The diversity

in the composition and biological activity of exosomes are induced by different extracellular environments or different physiological or pathological states of the secreting cells. Intermittent hypoxia results in a significant increase in the number of circulating exosomes, alters their miRNA cargo and function, such as inducing endothelial dysfunction [23]. The ability of plasma exosomes from remote ischemic preconditioning rats to attenuate cardiomyocytes apoptosis induced by I/R via transferring miR-24 has been confirmed [24]. Serum-derived exosomes from hepatic I/R challenged rats can cross the blood–brain barrier and mediate hippocampal and cortical neuronal pyroptosis [25]. Previously, we successfully isolated extracellular vesicles from intestinal tissues [26]. We found that extracellular vesicles from sham and intestinal I/R surgery had similar shapes and sizes, and our analysis of the RNA content of extracellular vesicles showed that small RNAs comprise the majority of the vesicles but carry remarkably different miRNAs [26].

Macrophages in the liver account for the largest fraction of all solid organs. The resident hepatic macrophages, referred to as Kupffer cells, are seeded along with sinusoidal endothelial cells and are pivotal killers that can constantly clear gut-originated pathogens from the blood to maintain the homeostatic function of the liver. It is well-known that macrophages are the main target cells of exosomes. Red blood cell-derived hemoglobin containing vesicles from the circulation was extensively and rapidly removed by Kupffer cells [27]. Moreover, PKH26-labeled exosomes from murine melanoma B16BL6 cells administered to mice via the tail vein were mainly taken up by macrophages in the liver and spleen [28]. Consistent with previous studies, our current results showed that gut-derived exosomes were internalized by RAW 264.7 macrophages *in vitro* and were primarily taken up by macrophages in the liver *In vivo*.

Macrophages are also pivotal for sensing tissue injury by recognizing danger-associated molecular patterns, which drive their activation. Activated macrophages are usually classically defined as M1 and M2 activated macrophages [29]. Excessive M1 macrophages in the injured liver are thought to be the source of pro-inflammatory cytokines, which enhance cell apoptosis and tissue damage [6]. Liver diseases are associated with the transfer of exosomes to macrophages. Exosomes derived from cholesterol-loaded hepatocytes can promote M1 macrophage polarization and induce an inflammatory response [30]. Similarly, in nonalcoholic fatty liver disease, hepatocyte-derived exosomal miR-192-5p degraded the mRNA of Rictor and subsequently downregulated the protein levels of p-Akt and p-FoxO1 in macrophages, which promoted M1 polarization and induced lipotoxic liver injury [31]. Based on these reports, we postulated that exosomes carrying the signals of intestinal I/R could target hepatic macrophages to induce liver injury. Our study showed that intestinal exosomes from intestinal I/R could trigger pro-inflammatory signaling and cytokine expression in RAW 264.7 macrophages *in vitro*. The effects of intestinal exosomes on hepatic macrophages *In vivo* were confirmed. We found that the injection of IR-Exo remarkably increased macrophage infiltration, the M1-type marker content, the number of M1-type macrophages, the ratio of M1/M2 macrophages, and M1 proinflammatory cytokines.

Clodronate liposomes have been reported to effectively deplete macrophages in the liver. In the hepatic I/R model, macrophage exhaustion with pretreatment of clodronate liposomes led to the amelioration of affected lesions in the liver [32]. Our study showed that the depletion of macrophages mitigated disordered hepatic architecture and liver dysfunction and increased gene expression of the M1 marker in the liver after intestinal I/R. Intriguingly, macrophage elimination also improved these exacerbated impairments in the liver induced by IR-Exo. These results further confirm that hepatic M1 macrophage polarization is responsible for gut-derived exosomes mediating liver injury after intestinal I/R.

GW4869, a noncompetitive inhibitor of membrane-neutral sphingomyelinase, has been reported to markedly reduce exosome release [33, 34]. We observed that GW4869 administration remarkably decreased the number of infiltrating macrophages in the damaged liver after intestinal I/R, the expression of CCL2, which is the major cytokine that recruits macrophages as well as other M1 cytokines, the proportion of M1-type macrophages, and the M1/M2 ratio of macrophages. GW4869-mediated blockade of exosome generation improved survival and alleviated intestinal I/R-triggered liver injury. Additionally, injecting IR-Exo in healthy mice resulted in liver injury similar to that observed with intestinal I/R. These results further confirm the potential role of exosomes in liver injury after intestinal I/R injury.

Communication between the gut and liver has a central role in the progression of diseases. Gut-derived toxins, gut microbiota, and their metabolites influence liver pathology. Other studies of the condition of intestinal mucosal damage have reported gut-derived exosomes carrying HMGB1 to reach the liver, leading to nonalcoholic fatty liver disease [35]. Our study also indicates that

intestinal exosomes act as a mediator between the gut and liver and polarize hepatic macrophages toward the M1 state in the pathophysiological process of intestinal I/R.

This study had some limitations. First, the critical components of exosomes as an endogenous danger signal molecule directly mediate liver injury after intestinal I/R; this will be investigated in a future study. Second, whether other important immune effector cells, such as neutrophils, T cells, and natural killer cells, may also be involved in exosome-mediated liver damage remains unknown. Third, parameters at varying periods and continuous gradient doses for exosomes could reflect more dynamic progression in the liver after intestinal I/R.

In conclusion, our study demonstrated that gut-derived exosomes induce liver injury after intestinal I/R by promoting hepatic M1 macrophage polarization and acting as a mediator in the gut-liver axis in the context of intestinal I/R-triggered hepatic injury. Therefore, inhibition of exosome secretion or suppression of macrophage activation could be therapeutic targets to prevent hepatic impairment after intestinal I/R.

SUPPLEMENTARY INFORMATION

The online version contains supplementary material available at https://doi.org/10.1007/s10753-022-01695-0.

ACKNOWLEDGEMENTS

We thank all the funds mentioned above for their support.

AUTHOR CONTRIBUTION

Study conception/design: Jin Zhao, Ke-Xuan Liu, Cai Li. Conduct of experiments: Jin Zhao, Xiao-Dong Chen. Data analysis: Jin Zhao, Zhengzheng Yan, Cai Li. Drafting of paper: Jin Zhao. Editing/revision of paper: Cai Li, Ke-Xuan Liu. Reading and approval of the final version of the paper: all authors

FUNDING

This work was supported by grants from National Natural Science Foundation, Beijing, China (81871609 to Cai Li, 81671955 to Ke-Xuan Liu), Key Program of National Natural Science Foundation, Beijing, China (81730058 to Ke-Xuan Liu).

DATA AVAILABILITY

The data that support the findings of this study are available on request from the corresponding author.

DECLARATIONS

Ethics Approval This study was approved by the Institutional Animal Care and Use Committee of Southern Medical University (Application number: NFYY-2018–0013).

Consent for Publication All authors have agreed for the publication of this paper.

Competing Interests The authors declare no competing interests.

REFERENCES

1. Zhan, Y., Y. Ling, Q. Deng, Y. Qiu, J. Shen, H. Lai, *et al*. 2022. HMGB1-Mediated Neutrophil Extracellular Trap Formation Exacerbates Intestinal Ischemia/Reperfusion-Induced Acute Lung Injury. *Journal of Immunology* (Baltimore, Md : 1950) 208: 968–978.
2. Zhang, Y.N., Z.N. Chang, Z.M. Liu, S.H. Wen, Y.Q. Zhan, H.J. Lai, *et al*. 2022. Dexmedetomidine Alleviates Gut-Vascular Barrier Damage and Distant Hepatic Injury Following Intestinal Ischemia/Reperfusion Injury in Mice. *Anesthesia and Analgesia* 134: 419–431.
3. Hu, J., F. Deng, B. Zhao, Z. Lin, Q. Sun, X. Yang, *et al*. 2022. Lactobacillus murinus alleviate intestinal ischemia/reperfusion injury through promoting the release of interleukin-10 from M2 macrophages via Toll-like receptor 2 signaling. *Microbiome* 10: 38.
4. Gonzalez, L., A. Moeser, and A. Blikslager. 2015. Animal models of ischemia-reperfusion-induced intestinal injury: Progress and promise for translational research. *American Journal of Physiology Gastrointestinal and Liver Physiology* 308: G63-75.
5. Horie, Y., R. Wolf, J. Russell, T. Shanley, and D. Granger. 1997. Role of Kupffer cells in gut ischemia/reperfusion-induced hepatic microvascular dysfunction in mice. *Hepatology (Baltimore, MD)* 26: 1499–1505.
6. Tacke, F. 2017. Targeting hepatic macrophages to treat liver diseases. *Journal of Hepatology* 66: 1300–1312.
7. Wen, S., X. Li, Y. Ling, S. Chen, Q. Deng, L. Yang, *et al*. 2020. HMGB1-associated necroptosis and Kupffer cells M1 polarization underlies remote liver injury induced by intestinal ischemia/reperfusion in rats. *FASEB journal : Official publication of the Federation of American Societies for Experimental Biology* 34: 4384–4402.
8. Mallegol, J., G. Van Niel, C. Lebreton, Y. Lepelletier, C. Candalh, C. Dugave, *et al*. 2007. T84-intestinal epithelial exosomes bear MHC class II/peptide complexes potentiating antigen presentation by dendritic cells. *Gastroenterology* 132: 1866–1876.
9. Kojima, M., J. Gimenes-Junior, T. Chan, B. Eliceiri, A. Baird, T. Costantini, *et al*. 2018. viaExosomes in postshock mesenteric lymph are key mediators of acute lung injury triggering the macrophage activation Toll-like receptor 4. *FASEB journal : Official publication of the Federation of American Societies for Experimental Biology* 32: 97–110.

10. Kojima, M., T. Costantini, B. Eliceiri, T. Chan, A. Baird, and R. Coimbra. 2018. Gut epithelial cell-derived exosomes trigger post-trauma immune dysfunction. *The Journal of Trauma and Acute Care Surgery* 84: 257–264.
11. Deng, Z., X. Zhuang, S. Ju, X. Xiang, J. Mu, Y. Liu, *et al*. 2013. Exosome-like nanoparticles from intestinal mucosal cells carry prostaglandin E2 and suppress activation of liver NKT cells. *Journal of Immunology* (Baltimore, Md : 1950) 190: 3579–89.
12. Jiang, L., Y. Shen, D. Guo, D. Yang, J. Liu, X. Fei, *et al*. 2016. EpCAM-dependent extracellular vesicles from intestinal epithelial cells maintain intestinal tract immune balance. *Nature Communications* 7: 13045.
13. Li, Y., Y. Cao, J. Xiao, J. Shang, Q. Tan, F. Ping, *et al*. 2020. Inhibitor of apoptosis-stimulating protein of p53 inhibits ferroptosis and alleviates intestinal ischemia/reperfusion-induced acute lung injury. *Cell Death and Differentiation* 27: 2635–2650.
14. Turnage, R., K. Kadesky, S. Myers, K. Guice, and K. Oldham. 1996. Hepatic hypoperfusion after intestinal reperfusion. *Surgery* 119: 151–160.
15. Okada, M., L. Falcão, D. Ferez, J. Martins, P. Errante, F. Rodrigues, *et al*. 2017. Effect of atenolol pre-treatment in heart damage in a model of intestinal ischemia-reperfusion. *Acta Cirúrgica Brasileira* 32: 964–972.
16. Chen, R., Z. Zeng, Y. Zhang, C. Cao, H. Liu, W. Li, *et al*. 2020. Ischemic postconditioning attenuates acute kidney injury following intestinal ischemia-reperfusion through Nrf2-regulated autophagy, anti-oxidation, and anti-inflammation in mice. *FASEB journal : Official publication of the Federation of American Societies for Experimental Biology* 34: 8887–8901.
17. Zhou, J., W. Huang, C. Li, G. Wu, Y. Li, S. Wen, *et al*. 2012. Intestinal ischemia/reperfusion enhances microglial activation and induces cerebral injury and memory dysfunction in rats. *Critical Care Medicine* 40: 2438–2448.
18. Hayase, N., K. Doi, T. Hiruma, R. Matsuura, Y. Hamasaki, E. Noiri, *et al*. 2019. Recombinant Thrombomodulin on Neutrophil Extracellular Traps in Murine Intestinal Ischemia-Reperfusion. *Anesthesiology* 131: 866–882.
19. Fan, X., J. Du, M. Wang, J. Li, B. Yang, Y. Chen, *et al*. 2019. Irisin Contributes to the Hepatoprotection of Dexmedetomidine during Intestinal Ischemia/Reperfusion. *Oxidative Medicine and Cellular Longevity* 2019: 7857082.
20. Zhao, H., F. Zhang, G. Shen, Y. Li, Y. Li, H. Jing, *et al*. 2010. Sulforaphane protects liver injury induced by intestinal ischemia reperfusion through Nrf2-ARE pathway. *World Journal of Gastroenterology* 16: 3002–3010.
21. Han, S., H. Li, M. Kim, V. D'Agati, and H. Lee. 2019. Intestinal Toll-like receptor 9 deficiency leads to Paneth cell hyperplasia and exacerbates kidney, intestine, and liver injury after ischemia/reperfusion injury. *Kidney International* 95: 859–879.
22. Horie, Y., R. Wolf, M. Miyasaka, D. Anderson, and D. Granger. 1996. Leukocyte adhesion and hepatic microvascular responses to intestinal ischemia/reperfusion in rats. *Gastroenterology* 111: 666–673.
23. Khalyfa, A., C. Zhang, A.A. Khalyfa, G.E. Foster, A.E. Beaudin, J. Andrade, *et al*. 2016. Effect on Intermittent Hypoxia on Plasma Exosomal Micro RNA Signature and Endothelial Function in Healthy Adults. *Sleep* 39: 2077–2090.
24. Minghua, W., G. Zhijian, H. Chahua, L. Qiang, X. Minxuan, W. Luqiao, *et al*. 2018. Plasma exosomes induced by remote ischaemic preconditioning attenuate myocardial ischaemia/reperfusion injury by transferring miR-24. *Cell death & disease* 9: 320.
25. Zhang, L., H. Liu, L. Jia, J. Lyu, Y. Sun, H. Yu, *et al*. 2019. Exosomes Mediate Hippocampal and Cortical Neuronal Injury Induced by Hepatic Ischemia-Reperfusion Injury through Activating Pyroptosis in Rats. *Oxidative medicine and cellular longevity* 2019: 3753485.
26. Chen, X., J. Zhao, Z. Yan, B. Zhou, W. Huang, W. Liu, *et al*. 2020. Isolation of extracellular vesicles from intestinal tissue in a mouse model of intestinal ischemia/reperfusion injury. *BioTechniques* 68: 257–262.
27. Willekens, F., J. Werre, J. Kruijt, B. Roerdinkholder-Stoelwinder, Y. Groenen-Döpp, A. van den Bos, *et al*. 2005. Liver Kupffer cells rapidly remove red blood cell-derived vesicles from the circulation by scavenger receptors. *Blood* 105: 2141–2145.
28. Imai, T., Y. Takahashi, M. Nishikawa, K. Kato, M. Morishita, T. Yamashita, *et al*. 2015. Macrophage-dependent clearance of systemically administered B16BL6-derived exosomes from the blood circulation in mice. *Journal of extracellular vesicles* 4: 26238.
29. Sica, A., M. Erreni, P. Allavena, and C. Porta. 2015. Macrophage polarization in pathology. *Cellular and molecular life sciences : CMLS* 72: 4111–4126.
30. Zhao, Z., L. Zhong, P. Li, K. He, C. Qiu, L. Zhao, *et al*. 2020. Cholesterol impairs hepatocyte lysosomal function causing M1 polarization of macrophages via exosomal miR-122-5p. *Experimental Cell Research* 387: 111738.
31. Liu, X., Q. Pan, H. Cao, F. Xin, Z. Zhao, R. Yang, *et al*. 2020. Lipotoxic hepatocyte-derived exosomal MicroRNA 192–5p Activates macrophages through rictor/Akt/forkhead box transcription factor O1 signaling in nonalcoholic fatty liver disease. *Hepatology (Baltimore, MD)* 72: 454–469.
32. Xiaoming, A., J. Wenbo, W. Jinyi, W. Bin, H. Chunyang, C. Qi, *et al*. 2020. Macrophage regnase-1 deletion deteriorates liver ischemia/reperfusion injury through regulation of macrophage polarization. *Frontiers in Physiology* 11: 582347.
33. Catalano, M., and L. O'Driscoll. 2020. Inhibiting extracellular vesicles formation and release: A review of EV inhibitors. *Journal of extracellular vesicles* 9: 1703244.
34. Essandoh, K., L. Yang, X. Wang, W. Huang, D. Qin, J. Hao, *et al*. 2015. Blockade of exosome generation with GW4869 dampens the sepsis-induced inflammation and cardiac dysfunction. *Biochimica et Biophysica Acta* 1852: 2362–2371.
35. Chen, Y., H. Sun, Y. Bai, and F. Zhi. 2019. Gut dysbiosis-derived exosomes trigger hepatic steatosis by transiting HMGB1 from intestinal to liver in mice. *Biochemical and Biophysical Research Communications* 509: 767–772.